INFERRING GLOBAL PATTERNS OF LUNAR SURFACE MINERALOGY FROM ELEMENTAL ABUNDANCE DATA USING ARTIFICIAL NEURAL NETWORKS. Y. Zhao[1], M. Laneuville[2], N. Guttenberg[2] and W. van Westrenen[1] [1]Faculty of Science, Vrije Universiteit Amsterdam, the Netherlands, [2]Earth-Life Science Institute, Tokyo Institute of Technology, Tokyo, Japan, email: y.zhao@vu.nl

Summary: We use novel machine learning techniques to infer global patterns of lunar surface mineralogy from elemental abundance data. We explore the information content in the distribution of the chemical elements in relation to each other, and discuss how they can be linked to the formation of common minerals in various surface regions. We independently confirm the global patterns of plagioclase and olivine distribution in Lemelin et al. (2016) [1].

Introduction: Global surface mineralogical maps are both valuable to understand the processes that shaped the crust and challenging to obtain due to the degeneracy between elements and minerals. Previous estimates of large-scale lunar surface mineralogy are typically obtained by using visible and near-infrared spectroscopy, multispectral imaging, and thermal emission spectroscopy [1-3]. We explore patterns in elemental abundance data directly to further constrain large-scale distributions of major minerals on the Moon.

We train an artificial neural network to predict the conditional probability of an element having a given abundance *y* given one or more element abundances at that point *x* (written p(y|x)). Where a common factor influences both the input(s) and output values, the prediction is expected to be good. By comparing the accuracy of the prediction to the case where the neural network learns p(y) without any other elemental knowledge, we can quantify the information gain obtained by the knowledge of *x* in terms of a *predictability* variable (written P(-) below).

We use this predictability analysis to explore regions in which certain elements are influenced by a common chemical process (e.g. formation of a specific mineral), without prior assumptions about correlations between the elements. This serves as an independent way to identify patterns in global mineralogical distribution, and infer geological processes.

Method: All data used are publicly available on the PDS website (https://pds.nasa.gov/). The elemental abundance data were obtained from the Gamma Ray and Neutron Spectrometer in the Lunar Prospector mission. Level 2 data were used. They include Mg, Al, Si, Ca, Ti, Fe content in the form of oxide weight fraction, and K, Th, U content in ppm. These data are binned on 2 degree equal area pixels. All data channels are normalized by their corresponding mean and standard deviation values.

At each pixel location, we construct a vector of all elemental abundance data, without spatial information. Train and test set are constructed by (1), randomizing the sequence of pixels so that spatial correlation is prevented and (2), dividing the domain into 4 sets of data, each of them rotating to be the test set while the other 3 serve as the training set.

We train a neural network to learn the conditional probability of each element abundance given the knowledge of one or more of the other abundances by minimizing the categorical cross-entropy loss (up to 49 one-to-one pairs, plus a few specific many-to-one networks as discussed below). The architecture is 5 layers deep and includes 25% dropouts between layers. It is implemented using the standard *torch* package in Python [4].

Once those predictive networks are trained, we compute a *predictability* metric P designed to show the percentage of information gained about the distribution of an element by adding the knowledge of another one. To do so, we compare the categorical cross-entropy loss predicting p(y) to that predicting p(y|x), normalizing it to the total entropy of y. The final number is between zero and one, with P = 1 being 'perfect predictability' (i.e., knowledge of *x* is equivalent to knowledge of *y*) and P = 0 being 'total independence' (where the knowledge of *x* does help predicting *y* at all). Given the fluctuations in the training of neural networks, only predictabilities higher than 0.1 are considered significant

We assume here that the process that influences how elements may be related to each other is the formation of minerals. We analyze the distributions of relative abundances of minerals, based on the predictability results. We take into account the common lunar minerals plagioclase, pyroxene, olivine, and ilmenite.

Results and interpretations: *1. Global distribution of plagioclase.* Fig 1a shows Ca content plotted against Al for the entire lunar surface. In particular, red color corresponds to the anorthositic crust. We can see that in the anorthositic crust, a broad inverse relation can be observed between Ca and Al, due to the high concentration of plagioclase in these areas. In the mare regions and SPA (green points), the range of Ca values is similar to that of highlands, but Al values can be very low. This shows that Ca- and Al-bearing pyroxene is present in these areas. In these areas, no clear inverse correlation can be observed between Ca and Al in Fig 1a. In fact, both P(Ca|Al) and P(Al|Ca) (Fig 2) are very

poor in these areas, and fall below the 0.1 threshold. The fact that P(Ca|Al) and P(Al|Ca) are virtually the same indicates that the neural network only modeled the inverse relation between Ca and Al in plagioclase, and did not find a pattern for Ca-Al relation in the mares. It follows that the regions that show predictability between Al and Ca are those where there is a significant amount of plagioclase. Our prediction of the distribution of plagioclase agrees with Lemelin et al. (2016) [1].

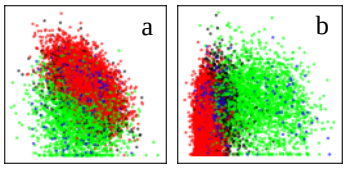

Figure 1. Left: global Ca content (x axis) plotted against Al. Right: global Fe content (x axis) plotted against Mg. All data are normalized by their mean and standard deviation. Red color corresponds to values from the anorthositic crust. Green color corresponds to mare regions and SPA.

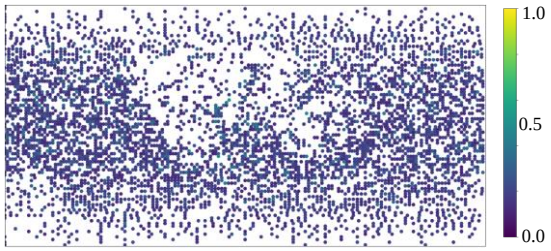

Figure 2. Predictability P(Al|Ca) with a 0.1 cut-off (see text). Map is centered along the Moon's prime meridian.

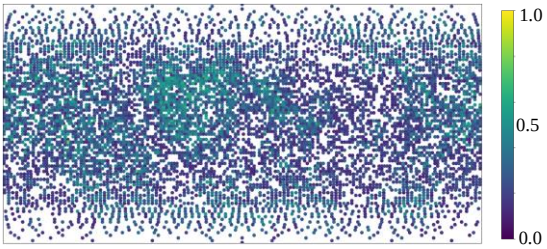

Figure 3. Predictability P(Fe|{Mg,Al}) with a 0.1 cut-off.

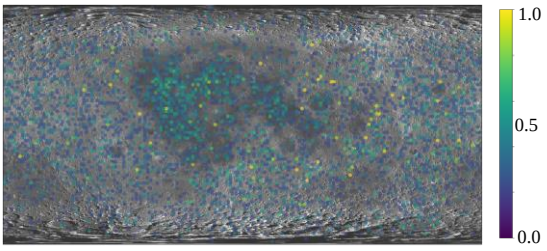

Figure 4. Location of olivine as predicted by P(Fe|{Mg,Al}) – P(Fe|Mg) with a 0.2 cut-off (see text). A lunar surface background is added to help identify locations.

2. Global distribution of olivine. P(Fe|Mg) is relatively good in the mare region, where there are high levels of mafic minerals. It is also relatively good in the highlands due to the very low Fe content (Fig 1b), which makes prediction easy without having to have a clear Mg-Fe relation. The prediction of Fe improves as we add the information of Al (i.e., P(Fe|{Mg,Al})), see Fig 3). Since Al is a good indicator of plagioclase, it informs the neural networks of the distribution of plagioclase, and by inference, the distribution of its counterpart: mafic minerals. Where the mafic minerals consist primarily of only Fe and Mg, the P(Fe|{Mg,Al}) is expected to be high. Since olivine contains far less Ca and Al, the P gain from P(Fe|Mg) to P(Fe|{Mg,Al}) is mainly due to the large presence of olivine. Fig 4 shows P(Fe|{Mg,Al}) – P(Fe|Mg) where its value is higher than 0.2. These are the areas where we expect to find relatively high concentrations of olivine.

3. Global distribution of pyroxene. Pyroxenes are the most complex mineral in terms of their chemical variability. Since most pyroxenes contain at least a few percent of other elements (Ca, Al, Ti, etc.), where P(Fe|{Mg,Al}) is poor (Fig 3), it indicates the presence of pyroxene. This does not include the small amount of pyroxenes containing virtually only Fe, Mg, Si and O. Many pairs of P from inputs with and without Ca are compared. Most of the time, the effect of adding Ca is rather small. We use P(Fe|{Mg,Al,Ca}) – P(Fe|{Mg,Al}) + P(Fe|{Ca,Al,Si}) – P(Fe|{Al,Si}) here to enhance the effect of Ca, and indicate the possible locations of high-Ca pyroxenes (Fig 5). A comparison between Fig 4 and 5 shows that the anorthositic crust of the near side contains mainly low-Ca pyroxene.

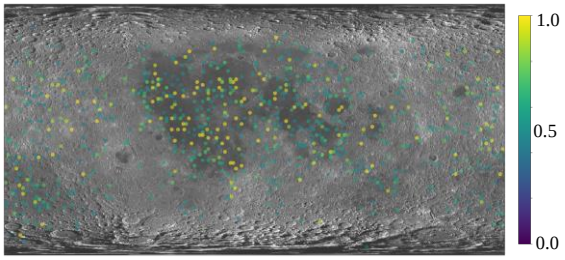

Figure 5. Possible location of high-Ca pyroxenes as predicted by P(Fe|{Mg,Al,Ca}) – P(Fe|{Mg,Al}) + P(Fe|{Ca,Al,Si}) – P(Fe|{Al,Si}) with a 0.4 cut-off.

Conclusions: We find that the global patterns of plagioclase and olivine distributions are in good agreement with Lemelin et al. (2016) [1]. We predict that high-Ca pyroxenes are distributed in relatively high amounts in the mare regions and SPA, whereas the near-side anorthositic crust contains mainly low-Ca pyroxenes.

References: [1] Lemelin M. et al. (2016) *LPSC XLVII*, Abstract #2994. [2] Tompkins S. and Pieters C. M. (1999) *Meteorit. Planet. Sci. 34*, 25. [3] Greenhagen B. T. et al. (2010) *Science 329*, 1507-1509. [4] Paszke et al. (2017) In *NIPS-W*.